Lower atmospheric anomalies following the 2008 Wenchuan Earthquake observed by GPS measurements

Shuanggen Jin [a,*], L. Han [a,c], J. Cho [b]

[a] Shanghai Astronomical Observatory, Chinese Academy of Sciences, Shanghai 200030, China
[b] Korea Astronomy and Space Science Institute, Daejeon 305-348, South Korea
[c] Graduate University of the Chinese Academy of Sciences, Beijing 100049, China

ABSTRACT

The Mw=8.0 Wenchuan Earthquake occurred on May 12, 2008 at the Longmen Shan fault, the western Sichuan Basin, China, killing more than ten thousand people in several cities and causing large economic losses. Global Positioning System (GPS) observations have provided unique insights on this event, including co-seismic ionospheric disturbances, co-/post-seismic crustal deformations and fault slip distributions. However, the processes and the driving mechanisms are still not clear, particularly possible seismo-lower atmospheric–ionospheric coupling behaviors. In this paper, the lower atmospheric (tropospheric) variations are investigated using the total zenith tropospheric delay (ZTD) from GPS measurements around this event. It has the first found co-seismic tropospheric anomalies during the mainshock with an increase and then a decrease, mainly in the zenith hydrostatic delay component (ZHD), while it is also supported by the same pattern of surface-observed atmospheric pressure changes at co-located GPS site that are driven by the ground-coupled air waves from ground vertical motion of seismic waves propagation. Therefore, the co-seismic tropospheric disturbances (CTD) indicate again the acoustic coupling effect of the atmosphere and the solid-Earth with air wave propagation from the ground to the top atmosphere.

1. Introduction

The Wenchuan earthquake with 8.0 Mw occurred at 14:28:01.42 CST (06:28:01.42 UTC) on May 12, 2008 in Sichuan province, West China. The extent of the earthquake and after shock-affected areas lie northeast, along the Longmen Shan fault, a thrust structure along the border of the Tibetan Plateau and the western Sichuan Basin. It was a deadly earthquake to hit China since the 1976 Tangshan Earthquake, which killed more than ten thousand people in several cities along the western Sichuan basin in China (Fig. 1). This event ruptured about 300 km of the Longmen Shan fault zone and lasted close to 120 s, with the majority of energy released in the first 80 s (Burchfiel et al., 2008; Toda et al., 2008; Parsons et al., 2008). The rupture started from the Wenchuan County and propagated at an average speed of 3.1 km/s, 49° toward northeast, rupturing a total of about 300 km (http://www.csi.ac.cn). Although robust seismic signals around the globe could help in estimating the gross nature of this event, the details of rupture are usually obscure due to the lack of near-field observations. Local

geodetic measurements can provide more details on the kinematic rupture and processes and the size of this continental event. For example, GPS observation results showed that co-seismic deformations move towards the earthquake epicenter and the largest magnitude is up to 2.3 m in the horizontal and 0.7 m in the vertical in Beichuan rather than in the epicenter (Jin et al., 2010).

Additionally, when GPS signals propagate through the atmosphere, they are delayed by the atmospheric (tropospheric and ionospheric) refraction, which results in lengthening of the geometric path of the ray, usually referred to as the tropospheric and ionospheric delays (e.g., Jin et al., 2004, 2006). The atmospheric delay disturbances may reflect the changes of the atmospheric compositions or air waves, e.g., acoustic wave propagation due to the movement of air particles. Numerous studies have found co-seismic or pre-seismic ionospheric anomalies and the speculated reason is the acoustic coupling of the atmosphere and the solid-Earth. For example, Jin et al. (2010) and Afraimovich et al. (2010) found significant co-seismic ionospheric total electron content (TEC) disturbances during the 2008 Wenchuan Earthquake as an intensive N-shape shock-acoustic wave with a plane waveform at half-period of about 200 s propagated towards northeast with a velocity 600 m/s from the epicenter, parallel to the rupture direction. The co-seismic TEC disturbance is possibly due to the coupling of the ionosphere and the solid-Earth with an air wave

* Corresponding author. Tel.: +86 21 64386191; fax: +86 21 64384618.
E-mail addresses: sgjin@shao.ac.cn, shuanggen.jin@gmail.com,
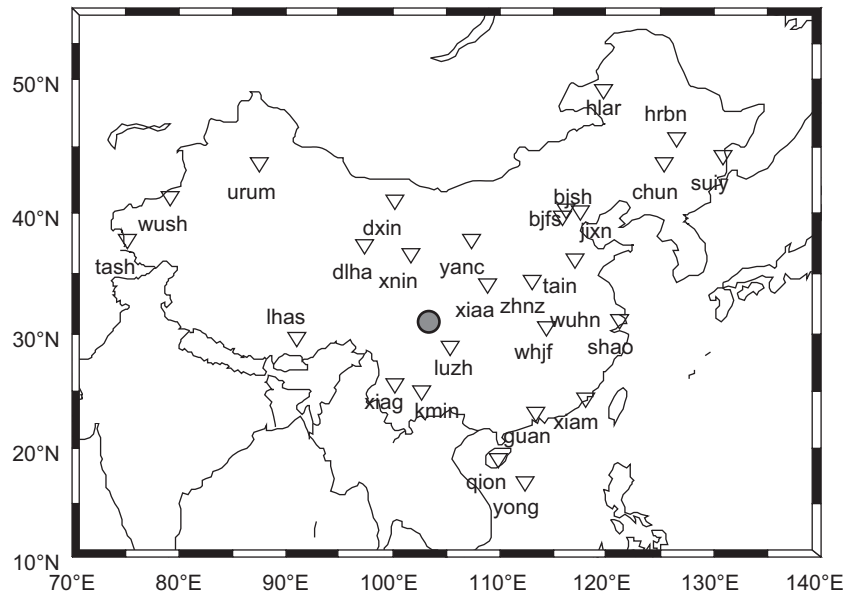sg.jin@yahoo.com (S. Jin).

Fig. 1. Distribution of GPS observation sites and the epicenter location of the May 12, 2008 Wenchuan Earthquake mainshock with about Mw 8.0. Triangles are the continuous GPS observing sites and large solid circles are the epicenter of the mainshock.

propagation from the ground to the ionosphere. If the air waves propagate from the ground to the top atmosphere, it may also affect the lower atmosphere (i.e. the troposphere). However, such possible impact on the troposphere has not been studied. In this paper, the possible tropospheric variations during the 2008 Wenchuan Earthquake are investigated for the first time using GPS network observation data collected from China national continuous and campaign GPS network. It further compared the data with surface atmospheric pressure observations at co-located GPS site and some possible mechanisms were finally discussed.

2. GPS observations and ZTD

The national project "Crustal Movement Observation Network of China (CMONC)" was initiated in August 1998 (Jin et al., 2010), including a nationwide fiducial network of 28 permanent GPS sites observed from August 1998 till date, and 56 survey mode sites with yearly operations for the period 1998–2008 as well as ~1000 regional campaign GPS stations operated by the State Bureau of Surveying and Mapping (SBSM) and the China Earthquake Administration (CEA) in 1999, 2001, 2004, 2007 and 2008, with at least 4-day observations in each session. Unfortunately, the observation data of only 28 continuous GPS sites are available around this event of May 12, 2008. Fig. 1 shows the continuous GPS site distribution, where the triangle stands for the continuous GPS observing sites and the large gray solid circle shows the epicenter of the mainshock.

The GPS observation data are processed by the GAMIT software (King and Bock, 1999), which solves the ZTD and other parameters using a constrained batch least squares inversion procedure. The International GNSS Service (IGS) final orbits, International Earth Rotation and Reference Systems Service (IERS) Earth orientation parameters and azimuth- and elevation-dependent antenna phase center models recommended by the IGS are used. The cut-off elevation angle is $15°$ and the temporal resolution of the ZTD estimate is 5 min. Since the GAMIT software parameterizes ZTD as a stochastic variation from the Saastamoinen model (Saastamoinent, 1973), with piecewise linear interpolation in between solution epochs, the GAMIT is very flexible to

allow *a priori* constraints of varying degrees of uncertainty. The variation from the hydrostatic delay is constrained to be a Gauss–Markov process with a specified power density of $2 \, \text{cm}/\sqrt{\text{h}}$, while the Gauss–Markov process provides an implicit constraint on the ZTD estimate at proceeding and following epochs, indicating that the accuracy is expected to be lower at the beginning and end of each window. In order not to degrade the accuracy of ZTD estimates, a 12 h sliding window strategy is designed and the ZTD is extracted from the middle 4 h of the window and then forward 4 h of moving window (Jin et al., 2007). Finally, the ZTD time series of several days around the mainshock are obtained at 28 continuous GPS sites in China with a temporal resolution of 5 min.

3. Results and discussion

Ionospheric disturbances during large earthquakes have been first found with the doppler sounding technique as the basal oscillation of the ionosphere (Yuen et al., 1969). Recently, GPS has successfully observed them as the perturbation in total electron content (TEC), number of electrons integrated along the line-of-sights. Numerous studies on ionospheric disturbances associated with seismic activities have been reported from GPS TEC. For example, Ducic et al. (2003) detected such a co-seismic ionospheric disturbance associated with 2002 Denali Earthquake, Alaska. Jin et al. (2010) found significant co-seismic ionospheric TEC disturbances with an intensive N-shape shock-acoustic wave propagation during the 2008 Wenchuan Earthquake. These ionospheric TEC disturbances associated with larger earthquakes are mainly due to the coupling of the ionosphere and the solid-Earth (Afraimovich et al., 2010). In a similar way, the coupling may also affect the lower atmosphere (i.e. the troposphere) as air waves propagate from the ground to the ionosphere. In the following, the possible tropospheric changes during the 2008 Wenchuan Earthquake are investigated by the total zenith tropospheric delay (ZTD) from dense GPS network observation data collected from China national continuous and campaign GPS network.

The daily ZTD time series with 5 min interval from 28 continuous GPS measurements in China are analyzed around the 12 May 2008 Wenchuan Earthquake. It is interesting to find

significant co-seismic tropospheric disturbance (CTD) in terms of ZTD near the epicenter. For example, Fig. 2 shows the daily ZTD residual time series at 5 min interval (ZTD minus the daily mean) from 11 to 13 May 2008 at Kmin site, southern part of the epicenter. The vertical dash line shows the mainshock time of the Wenchuan Earthquake and solid black line represents the ZTD residuals on May 12, 2008. The ZTD at the mainshock time (06:28 UTC, May 12, 2008) has a significant increase of about 15 mm, and then decrease after 2 h, while the ZTD on the non-earthquake days before and after May 12 has almost no anomaly changes. The ZTD variations at Lhas site, west of the epicenter, also show similar disturbances of about 10 mm increase and then decrease during the mainshock, while the ZTDs on the non-earthquake days before and after the earthquake also have no anomaly changes with a very consistent pattern, even two days prior or later (10 and 14 of May 2008; Fig. 3).

In addition, the independent Bernese software (Dach et al., 2007) is employed to process the raw GPS data. The new ZTD time series at 2 h interval are obtained at the 28 continuous GPS sites.
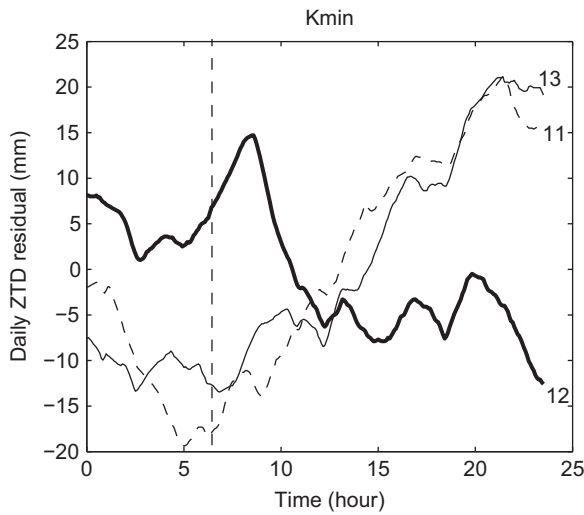

Fig. 4. Daily ZTD residual time series at 2 h interval from day 11 to 13 May 2008 at Kmin site. Vertical dash line shows the time of the Wenchuan Earthquake main-shock and solid black line represents the ZTD residuals on May 12, 2008.

Fig. 2. Daily 5 min ZTD residual time series (ZTD minus daily mean) from day 11 to 13 May 2008 at Kmin site. Vertical dash line shows the mainshock time of the Wenchuan Earthquake and solid black line represents the ZTD residuals on May 12, 2008.
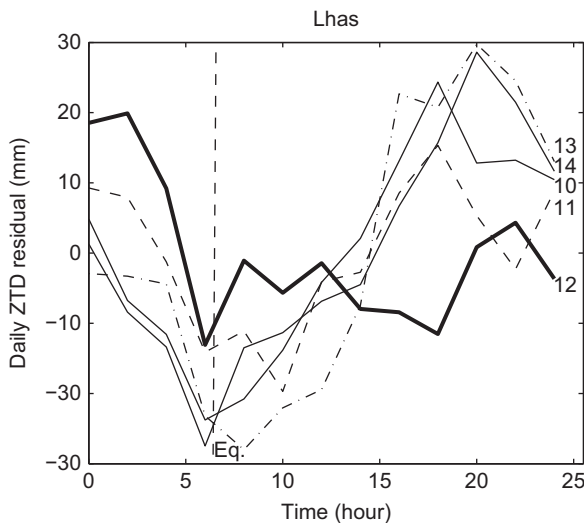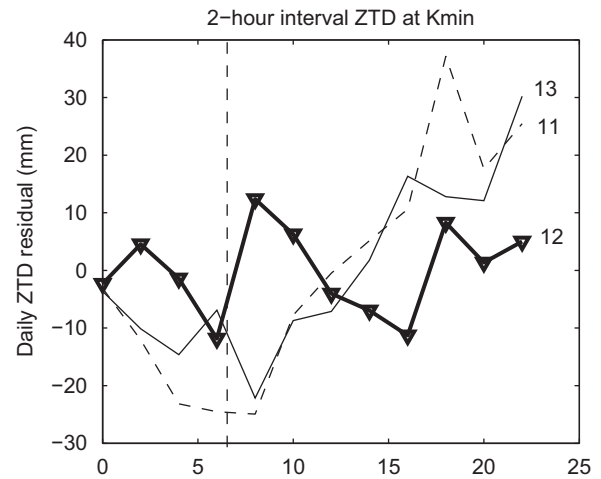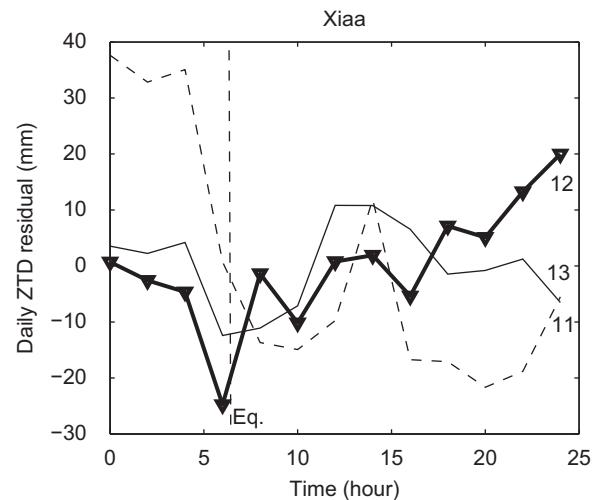

Fig. 5. Daily ZTD residual time series at 2 h interval from day 11 to 13 May 2008 at Xiaa site.

It showed similar co-seismic ZTD disturbances with the GAMIT processed results. For example, Fig. 4 shows the daily ZTD residuals at 2 h interval from day 11 to 13 May 2008 at Kmin site. The co-seismic ZTD disturbances at 2 h interval have almost the same as the 5 min ZTD time series variations during this earthquake (Fig. 2). The co-seismic ZTD at northern parts of the epicenter has similar increase and then decrease during the mainshock, e.g. at Xiaa (Fig. 5). Since there was no rain in these areas according to the Chinese Meteorological Administration during the daytime of May 12, 2008, the co-seismic ZTD anomalies during the event are mainly in the zenith hydrostatic delay component (ZHD). In addition, the effects on ZTD are reducing at the north part far from the epicenter, e.g., smaller co-seismic ZTD anomaly at the Xnin site (Fig. 6).

The available surface meteorological data at Lhas site are further analyzed and compared during this event. Fig. 7 shows the daily temperature residuals from day 11 to 13 May 2008 at Lhas site. The co-seismic temperature anomalies are found during the mainshock (Fig. 3), which may be caused due to rapid heating, releasing and then cooling during the earthquake (Tranmutoli et al., 2005). Furthermore, the atmospheric pressure has shown the same co-seismic ZTD disturbance pattern of increase and then decrease
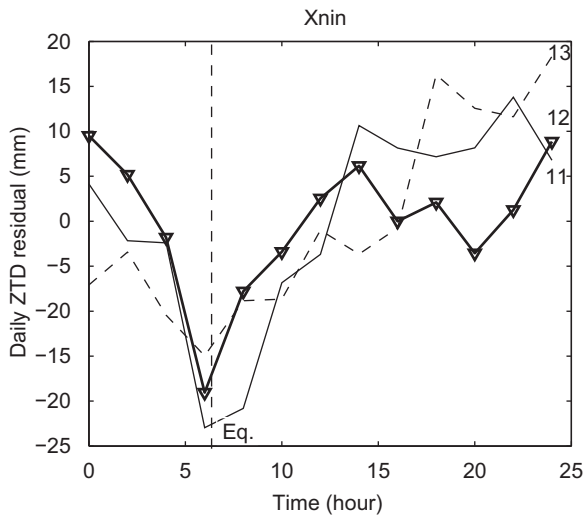

Fig. 3. Daily 5 min ZTD residual time series from day 10 to 14 May 2008 at Lhas site.

Fig. 6. Daily ZTD residual time series at 2 h interval from day 11 to 13 May 2008 at Xnin site.
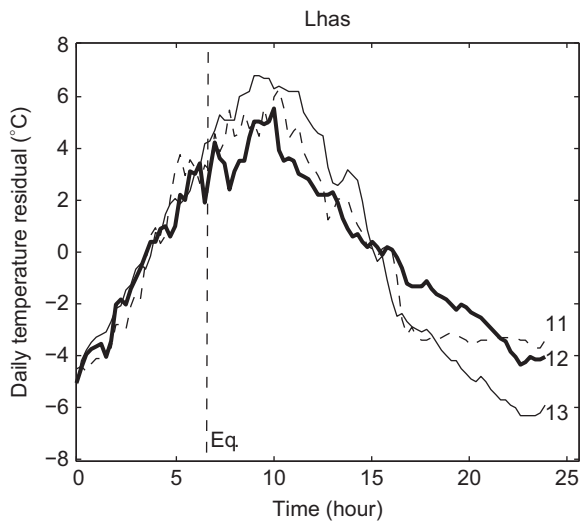

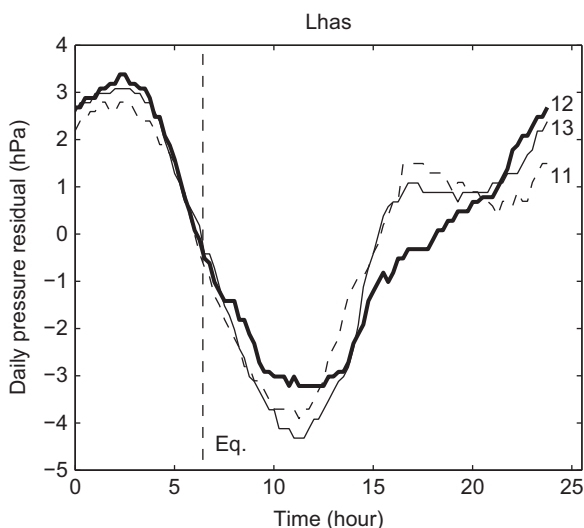**Fig. 7.** Daily temperature residuals from day 11 to 13 May 2008 at Lhas site.

Fig. 8. Daily pressure residuals from day 11 to 13 May 2008 at Lhas site.

during the mainshock at Lhas site (Fig. 8) as the ZTD disturbance (Fig. 3). Since the quick seismic surface waves propagation produces the radiated sound and infrasonic waves, these integrated interactions will generate ground-coupled air waves locally. The air waves propagate first upward or obliquely toward the upper atmosphere and after some time spread horizontally as acoustic-gravity waves in the lower atmosphere (Mikumo, 1968). The acoustic-gravity waves from the ground vertical motion will drive the atmospheric pressure disturbances (Watada et al., 2006). For example, Lighthill (1978) showed a simple relationship between the ground velocity and the pressure change at the surface as $\Delta p = \rho c_s w$, where $\Delta \rho$, ρ, c_s, and w are the pressure change, air density, sound velocity, and velocity of fluid motion, respectively.

Under the assumption of hydrostatic equilibrium, the change in pressure profile is related to the total density at altitude h through the approximate relationship as $dp = -\rho(h)g(h)dh$, where $\rho(h)$ and $g(h)$ are the density and gravity at the altitude h, respectively. Ignoring the change of gravity acceleration g with respect to height, the zenith hydrostatic delay (ZHD) can be expressed as (Saastamoinent, 1973), $ZHD = kp_0$, here k is a scale factor (2.28 mm/hPa) and p_0 is the pressure at height h_0 (Davis et al., 1985), namely $ZHD = 2.28p_0$. The hydrostatic component ZHD accounts for approximately 90% of ZTD, so ZTD is strongly correlated with surface pressure p_0 at the site. If surface pressure varies, the ZTD has a similar change with a scale factor of 2.28. Therefore the consistent co-seismic atmospheric pressure changes during the mainshock at Lhas site (Fig. 8) also support co-seismic tropospheric disturbances (CTD), mainly in the hydrostatic delay component (ZHD), which are driven by the acoustic coupling of the atmosphere and the solid-Earth with seismic waves propagating from the ground to the top atmosphere.

4. Conclusion

The violent earthquake of Mw 8.0 that occurred at the Longmen Shan fault zone was not expected, resulting in one of the largest death tolls during the last century as well as geologic damages. The GPS data provide detailed local insights on the earthquake, e.g., co-seismic ionospheric TEC disturbances due to possible seismo-tropospheric–ionospheric coupling (Jin et al., 2010; Afraimovich et al., 2010). Here, a significant co-seismic tropospheric disturbance (CTD) was found from GPS observations during the Wenchuan Earthquake. The ZTD at the mainshock time (06:28 UTC, May 12, 2008) has a change with increase and then decrease, while it is also supported by the surface observed atmospheric pressure change at co-located GPS site. Since there was no rain in these areas in the daytime of May 12, 2008, the co-seismic ZTD anomalies are mainly in the zenith hydrostatic delay component (ZHD). The co-seismic lower atmospheric disturbances are driven by the ground-coupled air waves from ground vertical motion of seismic waves propagation. Therefore, the co-seismic tropospheric delay disturbances (CTD) again show the acoustic coupling effect of the atmosphere and the solid-Earth with air wave propagation from the ground to the ionosphere. In future, further investigations of the lower atmospheric anomalies, coupling processes and mechanism between the lower atmosphere and the solid-Earth with more cases and observation data will be done.

Acknowledgements

References

Afraimovich, E., Feng, D., Kiryushkin, V., Astafyeva, E., Jin, S.G., Sankov, V., 2010. TEC response to the 2008 Wenchuan earthquake in comparison with other strong earthquakes. Int. J. Remote Sensing 31 (13), 3601–3613. doi:10.1080/01431161003727747.

Burchfiel, B.C., Royden, L.H., van der Hilst, R.D., et al., 2008. A geological and geophysical context for the Wenchuan earthquake of 12 May 2008, Sichuan, People's Republic of China. GSA Today 18 (7), 4–11.

Dach, R., Hugentobler, U., Fridez, P., Meindl, M., 2007. The Bernese GPS Software Version 5.0, University of Bern, Bern, Switzerland.

Davis, J.L., Herring, T.A., Shapiro, I., Rogers, A., Elgered, G., 1985. Geodesy by radio interferometry: effects of atmospheric modeling errors on estimates of baseline length. Radio Sci. 20 (6), 1593–1607.

Ducic, V., Artru, J., Longnonne, P., 2003. Ionospheric remote sensing of the Denali Earthquake Rayleigh surface wave. Geophys. Res. Lett. 30 (18), 1951. doi:10.1029/2003GL017812.

Jin, S.G., Wang, J., Zhang, H.P., Zhu, W.Y., 2004. Real-time monitoring and prediction of the total ionospheric electron content by means of GPS observations, Chin. Astron. Astrophys. 28 (3), 331–337. doi:10.1016/j.chinastron.2004.07.008.

Jin, S.G., Park, J., Wang, J., Choi, B., Park, P., 2006. Electron density profiles derived from ground-based GPS observations. J. Navig. 59 (3), 395–401. doi:10.1017/S0373463306003821.

Jin, S.G., Park, J.U., Cho, J.H., Park, P.H., 2007. Seasonal variability of GPS-derived Zenith Tropospheric Delay (1994–2006) and climate implications. J. Geophys. Res. 112, D09110. doi:10.1029/2006JD007772.

Jin, S.G., Zhu, W., Afraimovich, E., 2010. Co-seismic ionospheric and deformation signals on the 2008 magnitude 8.0 Wenchuan Earthquake from GPS observations. Int. J. Remote Sensing 31 (13), 3535–3543. doi:10.1080/01431161003727739.

King, R.W., Bock, Y., 1999. Documentation for the GAMIT GPS Analysis Software. Massachussetts Institute Technology, Cambridge, Massachussetts.

Lighthill, J., 1978. Waves in Fluids. Cambridge University Press, New York.

Mikumo, T., 1968. Atmospheric pressure waves and tectonic deformation associated with the Alaskan Earthquake of March 28, 1964. J. Geophys. Res. 73 (6), 2009–2025. doi:10.1029/JB073i006p02009.

Parsons, T., Ji, C., Kirby, E., 2008. Stress changes from the 2008 Wenchuan earthquake and increased hazard in the Sichuan basin. Nature 454, 509–510.

Saastamoinent, J., 1973. Contribution to the theory of atmospheric refraction. Bull. Geod. 107, 13–34.

Toda, S., Lin, J., Meghraoui, M., Stein, R.S.M., 2008. 12 May 2008 $M=7.9$ Wenchuan, China, earthquake calculated to increase failure stress and seismicity rate on three major fault systems. Geophys. Res. Lett. 35, L17305.

Tranmutoli, V., Cuomo, V., Filizzola, C., Pergola, N., Pietrapertosa, C., 2005. Assessing the potential of thermal infrared satellite surveys for monitoring seismically active areas: the case of Kocaeli (İzmit) earthquake, August 17, 1999. Remote Sensing Environ. 96, 409–426.

Watada, S., Kunugi, T., Hirata, K., Sugioka, H., Nishida, K., Sekiguchi, S., Oikawa, J., Tsuji, Y., Kanamori, H., 2006. Atmospheric pressure change associated with the 2003 Tokachi-Oki earthquake. Geophys. Res. Lett. 33, L24306. doi:10.1029/2006GL027967.

Yuen, P.C., Weaver, P.F., Suzuki, R.K., 1969. Continuous, traveling coupling between seismic waves and the ionosphere evident in May 1968 Japan earthquake data. J. Geophys. Res. 74, 2256–2264.